Published online 31 August 2009

Nucleic Acids Research, 2009, Vol. 37, No. 19 ***6355–6370***
doi:10.1093/nar/gkp700

CpG methylation potentiates pixantrone and doxorubicin-induced DNA damage and is a marker of drug sensitivity

Benny J. Evison[1], Rebecca A. Bilardi[1], Francis C. K. Chiu[2], Gabriella Pezzoni[3], Don R. Phillips[1] and Suzanne M. Cutts[1,*]

[1]Department of Biochemistry, La Trobe University, Victoria 3086, [2]Centre for Drug Candidate Optimisation, Monash Institute of Pharmaceutical Sciences, Monash University, Parkville, Victoria 3052, Australia and [3]Cell Therapeutics Europe, I-20091 Bresso, Italy

Received July 2, 2009; Revised and Accepted August 6, 2009

ABSTRACT

DNA methylation is an epigenetic modification of the mammalian genome that occurs predominantly at cytosine residues of the CpG dinucleotide. Following formaldehyde activation, pixantrone alkylates DNA and particularly favours the CpG motif. Aberrations in CpG methylation patterns are a feature of most cancer types, a characteristic that may determine their susceptibility to specific drug treatments. Given their common target, DNA methylation may modulate the DNA damage induced by formaldehyde-activated pixantrone. *In vitro* transcription, mass spectrometry and oligonucleotide band shift assays were utilized to establish that pixantrone–DNA adduct formation was consistently enhanced 2–5-fold at discrete methylated CpG doublets. The methylation-mediated enhancement was exquisitely sensitive to the position of the methyl substituent since methylation at neighboring cytosine residues failed to confer an increase in pixantrone–DNA alkylation. Covalent modification of DNA by formaldehyde-activated doxorubicin, but not cisplatin, was augmented by neighbouring CpG methylation, indicating that modulation of binding by CpG methylation is not a general feature of all alkylators. HCT116 colon cancer cells vastly deficient in CpG methylation were 12- and 10-fold more resistant to pixantrone and doxorubicin relative to the wild-type line, suggesting that these drugs may selectively recognize the aberrant CpG methylation profiles characteristic of most tumour types.

INTRODUCTION

Pixantrone is a novel aza-anthracenedione that was originally developed to improve the therapeutic profile of mitoxantrone, a DNA-interactive agent currently used in the clinical management of a range of haematological malignancies and solid tumours (1). Like mitoxantrone, pixantrone interacts with DNA via intercalation (2) and stimulates topoisomerase II-mediated DNA cleavage (3,4) presumably by stabilizing the cleavable complex (5). Despite the drug's ability to stimulate DNA cleavage via topoisomerase II impairment, this form of DNA damage does not directly correlate with drug cytotoxicity (3–5), suggesting that pixantrone may operate by a distinct, currently undefined mechanism of cell kill. A novel form of pixantrone–DNA interaction has recently emerged in which the drug can be extrinsically activated by formaldehyde to form covalent drug–DNA adducts (6). Formaldehyde-activated pixantrone exhibits considerable discrimination in alkylating DNA selectively at CpG and CpA dinucleotides via the terminal primary amino group of a single drug side-chain (7).

In addition to being a favoured target of formaldehyde-activated pixantrone, the CpG dinucleotide is unique in other respects. Globally, the mammalian genome comprises ~50 million CpG doublets (8) and therefore occurs well below its expected statistical frequency (8–11). The spatial distribution of CpG dinucleotides across the genome is uneven and non-random (10) and includes vast stretches of genomic DNA deficient in this specific doublet (8,10,12). These extensive stretches are punctuated by relatively small clusters of CpG sequences, ~1 kb in length, termed CpG islands (8,10–12). CpG islands are closely associated with regulatory promoter regions of many mammalian genes (9–13).

Although most CpG sequences are methylated in the mammalian genome, CpG islands harbour over 50% of

*To whom correspondence should be addressed. Tel: +61-03-9479-1517; Fax: +61-03-9479-2467; Email: s.cutts@latrobe.edu.au

all unmethylated CpG doublets (10), which essentially remain unmethylated throughout development in most tissues (10,11,14). Cytosine methylation typically occurs following DNA replication, predominantly by the maintenance methyltransferase DNMT1 (8,10,12). DNMT1 is responsible for the faithful transmission of CpG methylation patterns between cell generations by the post-replicative re-establishment of hemi-methylated CpG doublets to a fully methylated status (8,12,14) and CpG methylation patterns are actively maintained following each cell division.

DNA methylation assumes an important role in numerous physiological events that include embryonic development, genomic imprinting and X-inactivation by affording the cell an additional element of information storage without affecting the primary nucleotide sequence (8,14). Modification of the genome by methylation, particularly those CpG islands affiliated with imprinted genes and X chromosome inactivated genes, enables the stable transcriptional suppression of the associated gene (10,12,14). Recently, it has been established that numerous cancer-related genes can also be inactivated following the aberrant methylation of CpG islands in their promoter regions and this can have significant implications for the development of cancer (10–12,14). Cancer-specific methylation of CpG islands has been established in a range of tumour suppressor genes, DNA repair genes and genes that suppress angiogenesis, tumour invasion and metastasis (11,12,14).

An expanding list of genes that are susceptible to inactivation by aberrant hypermethylation has enabled investigators to analyse the patterns of silenced genes among different cancer types (15,16). Each tumour type has a distinctive profile of CpG island hypermethylation (15–19), which may facilitate the construction of a powerful set of biomarkers for tumour classification (19) and diagnostics (8,16). A prominent example is the hypermethylation-mediated inactivation of BRCA1, a DNA double strand break repair gene, which is frequently detected in breast and ovarian tumours, but not in other cancer types (16). Such a strong emphasis on cancer-specific, genome-wide CpG methylation profiling in recent times has seen the term cancer 'methylome' become fashionable (17).

DNA methylation profiling of cancers may also be used as a predictor for the susceptibility of a cancer to a specific drug treatment and this may have significant implications for drugs that target the CpG doublet (20,21). It is conceivable that CpG specific drugs, such as activated pixantrone, may recognize the aberrant methylation profiles that are characteristic of cancer cells. Perhaps more importantly, the methylation status of CpG dinucleotides may modulate the biological response to the drug. At a global level, DNA fragments methylated by SssI methylase are highly susceptible to adduct-induced duplex stabilization by formaldehyde-activated pixantrone (7). However, the effect of more localized CpG methylation on pixantrone–DNA interactions, namely at individual CpG doublets, has not been thoroughly characterized. Given the localized hypermethylation of CpG islands and the associated silencing of many cancer-related genes within neoplastic cells, the modulation of pixantrone–DNA interactions by methylation at localized CpG sequences was the primary focus of the present study.

MATERIALS AND METHODS

Materials

Pixantrone was kindly supplied by Cell Therapeutics Europe (CTE) (Bresso, Italy), while doxorubicin was a gift from Pfizer (Milan, Italy). Cisplatin and 3-(4,5-dimethyl-2-thiazolyl)-2,5-diphenyl-2H-tetrazolium bromide (MTT) were from Sigma Chemical Co, while formaldehyde was purchased from BDH. The DNA modifying enzymes HpaII methylase, HhaI methylase and MspI methylase were purchased from New England Biolabs. The restriction endonucleases HpaII, HhaI and MspI were obtained from Promega. All remaining chemicals and reagents were of analytical grade. Distilled water passed through a four-stage Milli-Q purification system (Millipore) was used to prepare all solutions.

Drugs

Stock solutions of pixantrone and doxorubicin were prepared by dissolving each in Milli-Q water to a final approximate concentration of 1–2 mM. The precise concentrations of each drug stock were determined spectrophotometrically using the extinction coefficients $\varepsilon^{1\%}_{1\,cm} = 296$ at 641 nm and $\varepsilon = 11\,500\,M^{-1}\,cm^{-1}$ at 480 nm for pixantrone and doxorubicin, respectively. Each drug stock was subsequently stored at −20°C. An accurately prepared mass of cisplatin was dissolved in 0.9% sodium chloride solution to generate a stock concentration of 1.58 mM. Cisplatin and formaldehyde solutions were prepared freshly on the day of each experiment.

DNA source

Plasmid pCC1 and the 512 bp fragment containing the *lac* UV5 promoter derived from the plasmid were prepared as described previously (6,7). The sequences of both unmethylated and methylated oligonucleotides (obtained from Geneworks) were: BE1, 5′-TTATTTCCG GCGCCTTATTT-3′; BE2, 5′-AAATAAGGCGCCGGA AATAA-3′; BE6, 5′-TTATTTCC^{Me}GGC^{Me}GCCTTAT TT-3′; and BE7, 5′-AAATAAGGC^{Me}GCC^{Me}GGAAAT AA-3′. C^{Me} represents the modified base 5-methylcytosine. The extinction coefficients for each oligonucleotide were determined using a formula provided by Wallace and Miyada (22).

Purification, labelling and annealing of oligonucleotides

Duplex oligonucleotides were prepared as described in Evison *et al.* (7). This protocol enabled the generation of four distinct duplexes including unmethylated dsBE12, hemi-methylated dsBE17 and dsBE26 and fully methylated dsBE67.

Methylation of DNA

The 512 bp fragment was incubated with HpaII methylase and 80 μM *S*-adenosyl-methionine at 37°C overnight. This reaction enabled the methylation of the internal cytosine residue of five independent 5′-CCGG-3′ sequences that occur within the 512 bp fragment. The methylation status of the fragment was confirmed by challenging the DNA with HpaII, an endonuclease that specifically cleaves DNA at unmethylated CCGG sites. Products of the restriction digest were separated and visualized electrophoretically, and in each case the 512 bp fragment remained intact, suggesting that the DNA was fully methylated.

In separate reactions, the 512 bp fragment was specifically methylated at either the external cytosine of the five CCGG sites or at the internal cytosine of four independent 5′-GCGC-3′ sequences using MspI methylase and HhaI methylase, respectively. Methylation of the fragment was confirmed by establishing that the modified sequences were resistant to cleavage by the appropriate restriction endonuclease. Both native (unmethylated) and methylated 512 bp fragments were used as templates for all subsequent transcription studies.

Drug reaction conditions

Generally, covalent drug–DNA adducts were generated in a reaction mixture consisting of the following: either native or methylated DNA was reacted with pixantrone or doxorubicin (together with formaldehyde) in phosphate buffered saline (PBS) (pH 7.0) at 37°C. The composition and conditions of each reaction were highly assay-dependent and are specified in the appropriate figure legend.

In vitro transcription assay

Drug-reacted DNA samples were typically processed and subjected to *in vitro* transcription assays as originally described (7). *In vitro* transcription samples were processed and electrophoresed through 12% denaturing polyacrylamide gels. Gels were subsequently fixed in 10% glacial acetic acid/10% methanol, dried, analysed by phosphorimaging and quantitated using ImageQuant software (Molecular Dynamics, CA).

Oligonucleotide band shift assay

Following reaction with pixantrone and formaldehyde, [^{32}P]-end labelled oligonucleotide samples were subjected to a gel shift assay as previously described (7). DNA adduct stability studies using the gel shift assay were performed in a similar manner, however two modifications to the procedure were introduced. Firstly, following the completion of each reaction, samples were passed through a Micro Bio-Spin 6 chromatography column to remove unreacted drug from the mix. Secondly, the purified samples were subsequently incubated at 37°C for defined time periods up to 3 h. Samples were then subjected to 19% denaturing PAGE overnight at 600 V at room temperature. Gels were subsequently fixed as described earlier, exposed to a Phosphor screen for 2 h and then analysed and quantitated as described previously.

Mass spectrometry studies

Oligonucleotide duplexes dsBE12 or dsBE67 were initially reacted with formaldehyde and pixantrone to yield a covalent pixantrone–DNA complex, which was subsequently purified by electrophoresis followed by electroelution. Initially, samples were directly loaded onto a cooled pre-electrophoresed 19% denaturing polyacrylamide gel (18 × 23 cm) and then subjected to electrophoresis at 4°C overnight at 300 V. Electrophoretic resolution of the covalent pixantrone–DNA complex yielded a blue band that was clearly visible to the naked eye. The blue band was subsequently excised from the gel with a clean scalpel and the pixantrone–DNA complex electroeluted from the gel slice using the Elutrap apparatus at 120 V for 3 h at 4°C. The purified covalent drug–DNA complex was subsequently subjected to centrifugation at 14°C for 2 h at 6500× *g* using a Centricon Centrifugal Filter Unit (MWCO 3 kDa) and then desalted four times into 10 mM ammonium acetate by gel filtration (Micro Bio-Spin 6 chromatography column). Mass spectrometric analysis of the drug–DNA complex was then carried out as described earlier (7).

Cell culture and growth inhibition assays

The human colorectal cancer cell line HCT116 and an isogenic derivative HCT116DKO (clone 1; deficient in DNMT1 and DNMT3b) were provided by Prof. Bert Vogelstein (John Hopkins University, MD, USA). Both cell lines were maintained in RPMI 1640 medium (Invitrogen) supplemented with 10% FCS (Trace Scientific) and grown in a humidified incubator at 37°C with 5% CO_2.

Growth inhibition was evaluated using an MTT assay. Cells were initially seeded at 3000 or 10 000 cells per well (HCT116 and HCT116DKO, respectively) into 96-well plates and allowed to attach for 24 h. Cells were treated with drug and incubated for a further 72 h. MTT was dissolved in PBS, sterile filtered and diluted to 1 mg/ml in serum-free culture medium. The MTT mix was added to cells (final concentration 0.33 mg/ml) and incubated for a further 2.5 h. Media was subsequently removed by aspiration and the insoluble MTT crystals dissolved in DMSO. Following reconstitution, the absorbance of MTT was measured at 570 nm. Drug concentrations inducing a level of 50% growth inhibition (IC_{50}) were determined using Microcal Origin software.

RESULTS

One of the most significant changes in the methylation pattern of a cancer cell is the local hypermethylation of CpG islands of many cancer-related genes (11,12,14). The *in vitro* transcription assay is an ideal system for investigating the effect of local CpG methylation on novel drug–DNA interactions given its ability to probe individual drug binding sites with exquisite sensitivity.

Consequently, *in vitro* transcription was initially used to examine the influence of CpG methylation on formaldehyde-activated pixantrone-induced DNA damage at discrete, localized CpG dinucleotides.

Localized CCm^{5}GG methylation by HpaII methylase enhances the generation of pixantrone–DNA adducts

Prior to transcription, a native, unmethylated 512 bp fragment containing the *lac* UV5 promoter was pre-reacted with 2 mM formaldehyde and increasing concentrations of pixantrone (0–10 μM). Each sample was subsequently subjected to transcription initiation by the addition of *Escherichia coli* RNA polymerase and the extension of each initiated transcript permitted by the addition of high concentrations of all four nucleotides. In the absence of pixantrone (lane 0, Figure 1A), the enzyme transcribes efficiently through the template to generate a full length RNA transcript 379 bases long. Importantly, no blockages are evident in this control (lane 0, Figure 1A), which suggests that formaldehyde alone does not induce transcriptional blockages. With increasing concentrations of pixantrone, RNA polymerase becomes increasingly blocked at specific sites (lanes 0.25–10, Figure 1A). The pattern of transcriptional blockages depicted in Figure 1A is consistent with the CpG and CpA selectivity of formaldehyde-activated pixantrone DNA adducts reported previously (7).

Multiple reactions containing 2 mM formaldehyde and pixantrone (0–10 μM) were run in parallel, however the native, unmethylated 512 bp fragment was substituted for an identical fragment methylated by HpaII methylase, an enzyme that transfers a methyl group to the internal cytosine residue of its target sequence CCGG (denoted CCm^{5}GG). Following transcription, HpaII-methylated DNA templates yielded a profile of drug-induced blockages (Figure 1B) identical in pattern to the transcriptional footprint induced using the unmethylated DNA template (Figure 1A). Although the pattern of blockages remains the same, there is a clear increase in the intensity of drug-induced blockages specifically at CCm^{5}GG sites originally methylated by HpaII methylase (indicated by sites X, Y and Z at the right of Figure 1B). The pixantrone-induced blockages at sites X, Y and Z were quantitated as a fraction of all transcripts in each lane and are represented as a function of pixantrone concentration in Figure 1C–E. These graphs show that pixantrone–DNA adduct formation is enhanced 2–3-fold at each of the three CCm^{5}GG sites relative to the corresponding unmethylated CCGG sequences (Figure 1C–E). As an internal control, the fraction of transcriptional blockages at an unmethylated CpG site was quantitated (indicated by CS at the right of Figure 1B, and shown in Figure 1F) and reveals that there was no significant difference in the generation of pixantrone–DNA adducts at unmethylated sites on either the native or methylated DNA template. Such a control indicates that the enhancement of pixantrone–DNA adducts occurs specifically at localized CCm^{5}GG sites and is not a general, non-specific event.

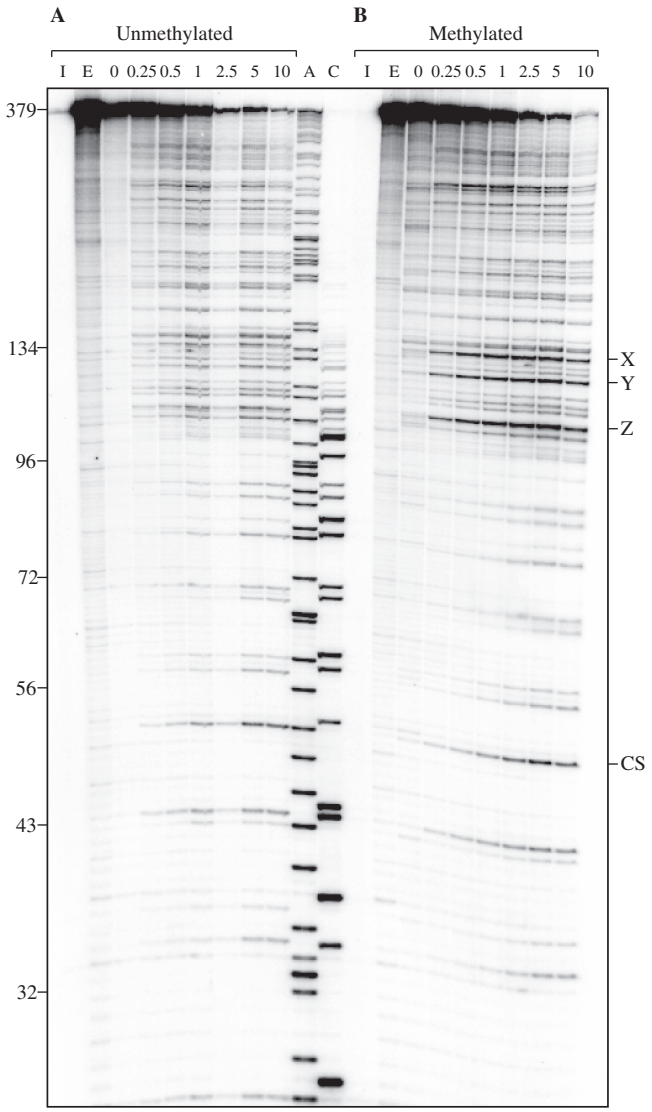

Figure 1. Drug-induced transcriptional blockages are enhanced at discrete HpaII-methylated sequences. (**A**) A 512 bp DNA fragment (25 μM_{bp}) containing the *lac* UV5 promoter was reacted with pixantrone (0–10 μM as indicated) and 2 mM formaldehyde for 4 h. Samples were subsequently ethanol precipitated, resuspended in transcription buffer and then subjected to transcription. Following initiation from the *lac* UV5 promoter, the transcription complex was elongated for 5 min and then terminated. Lanes I and E are controls representing an initiated complex that has not been elongated and extension of this complex to generate the full length transcript, respectively. Lanes A and C are sequencing lanes which were obtained using 3′-*O*-methoxy-ATP or 3′-*O*-methoxy-CTP during elongation, respectively. The length of selected transcripts is indicated at the left of the phosphorimage. (**B**) The native 512 bp fragment in (A) was substituted for an identical fragment specifically methylated by HpaII methylase at the internal cytosine of each CCGG recognition sequence. The methylated fragment was subsequently reacted with drug and subjected to transcription as described in (A). CCGG sites are indicated by X, Y and Z at the right of the phosphorimage, while CS denotes an unmethylated CpG site used as a control. The percentage of drug-induced blockages at native (solid squares) and methylated (open squares) sites X, Y and Z were quantitated as a fraction of each entire lane and are represented as a function of pixantrone concentration in (**C**), (**D**) and (**E**), respectively. (**F**) The percentage transcriptional blockage of the control site CS, a CpG site not methylated by HpaII methylase, was quantitated and is expressed as a function of pixantrone concentration.

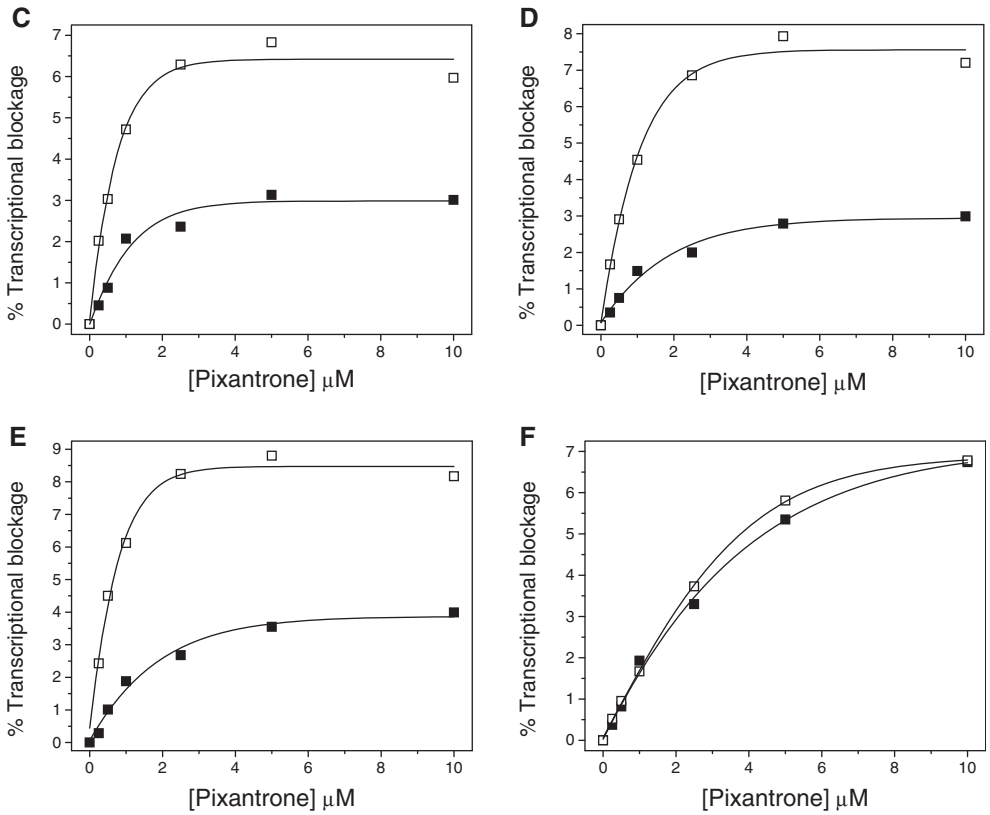

Figure 1. Continued.

Localized GCm^{5}GC methylation by HhaI methylase enhances the generation of pixantrone–DNA adducts

Given the enhancement of pixantrone–DNA adducts at CCm^{5}GG sequences, an alternative methylated sequence was selected to further characterize the role of methylation in the generation of pixantrone–DNA adducts. The 512 bp fragment was treated with HhaI methylase to specifically methylate the internal cytosine of the target sequence GCGC (denoted GCm^{5}GC). Following reaction of native and HhaI-methylated DNA templates with formaldehyde and pixantrone, each sample was subjected to transcription. A distinct increase in the intensity of pixantrone-induced blockages was evident at GCm^{5}GC sequences relative to unmethylated GCGC sites (Supplementary Figure S1). Quantitation of these specific blockages revealed a 2–3-fold increase in blockage frequency at GCm^{5}GC sites (Supplementary Figure S2), suggesting that methylation enhances pixantrone–DNA adducts at these sites.

Localized Cm^{5}CGG methylation by MspI methylase does not enhance the generation of pixantrone–DNA adducts

Having established that pixantrone–DNA adducts were specifically enhanced at discrete CCm^{5}GG sequences, it was of interest to probe the potential influence of cytosine methylation at other neighbouring residues. MspI methylase provided an ideal opportunity to investigate this idea given its ability to specifically methylate the external cytosine of CCGG (denoted Cm^{5}CGG). Both native and MspI-methylated DNA templates were prepared and reacted with formaldehyde and pixantrone to generate drug–DNA adducts as originally described. Drug-reacted templates were subjected to transcription and yielded the transcription footprint illustrated in Figure 2. Each of the pixantrone-induced blockages located at the three CCGG sites (indicated by sites X, Y and Z at the right of Figure 2B) were quantitated and are expressed as a function of pixantrone concentration in Figure 2C–E. Unlike HpaII methylation, Figure 2C–E indicates that Cm^{5}CGG methylation had no effect on the generation of pixantrone–DNA adducts at these sequences. The fraction of drug-induced transcriptional blockages was quantitated at an unmethylated CpG site (denoted CS at the right of Figure 2B). Figure 2F shows that there was no difference in the generation of pixantrone adducts at the unmethylated CpG site using the native DNA template versus the MspI-methylated template.

Formaldehyde-mediated alkylation of DNA by pixantrone is enhanced in synthetic oligonucleotides containing 5-methyl-deoxycytosine

Chemically-modified oligonucleotides were subsequently used to further evaluate the role of CpG methylation in the DNA binding of formaldehyde-activated pixantrone. Both native and methylated 5′-end labelled

oligonucleotides (25 μM_{bp}) were modified in a reaction mixture containing 2 mM formaldehyde and 0–50 μM pixantrone. Following an overnight incubation at 37°C, drug-reacted oligonucleotides were resolved by electrophoresis on a denaturing polyacrylamide gel. The resulting phosphorimage is presented in Figure 3A. The extent of adduct-induced stabilization of each oligonucleotide duplex, which is indicated by the uppermost band (Figure 3A), was quantitated and is presented as a function of pixantrone concentration in Figure 3B. The generation of drug-stabilized duplexes was strongly dependent on pixantrone concentration and there was a clear 2–5-fold enhancement in the alkylation of the fully methylated oligonucleotide dsBE67 (Figure 3B, solid line, open squares) relative to native duplex dsBE12 (Figure 3B, solid line, solid squares) throughout the range of pixantrone concentrations tested.

Given the highly amenable nature of oligonucleotide design, it was possible to construct two novel duplexes, in which only *one* of the strands was methylated. As substrates for alkylation by formaldehyde-activated pixantrone, these hemi-methylated duplexes were not as susceptible to adduct formation relative to the fully methylated oligonucleotide dsBE67 (Figure 3B, solid line, open squares), yet a moderate 1.25 to 2.5-fold increase in pixantrone adduct formation was observed within the hemi-methylated oligonucleotides dsBE17 and dsBE26 (Figure 3B, dashed line, open circles and dashed line, solid circles, respectively).

Mass spectrometric analysis of the covalent pixantrone–dsBE12 and pixantrone–dsBE67 complexes

The binding of formaldehyde-activated pixantrone to unmethylated duplex dsBE12 and fully methylated oligonucleotide dsBE67 was subsequently analysed by mass spectrometry. Reaction mixtures consisting of 100 μM pixantrone, 10 mM formaldehyde and either dsBE12 or dsBE67 (50 μM) were constructed and incubated at 37°C overnight. Drug–DNA complexes were subsequently processed using electrophoresis and electroelution as described in the 'Materials and Methods' section. Finally, samples were subjected to mass spectrometric analysis, which yielded the spectra presented in Figure 4. Mass spectrometric analysis of the dsBE12-pixantrone complex (Figure 4A) yielded a spectral pattern that was fully consistent with the presence of dsBE12 (peak 12 232 Da), dsBE12-intercalated pixantrone (peak 12 557 Da) and the dsBE12-pixantrone covalent adduct (peak 12 569 Da) and is summarized in Table 1.

Duplex dsBE67 was detected predominantly as a single peak (Figure 4B) associated with a mass of 12 291 Da, a value that compared favourably with the expected mass of the duplex (Table 1). A second key peak was evident at 12 615 Da, a mass that is consistent with a single pixantrone molecule intercalated within the duplex (Table 1). A third and very prominent peak was detected at 12 627 Da (Figure 4B), a mass which most likely reflects the addition of a single methylene unit (mediated by formaldehyde) to generate a single pixantrone–DNA adduct (Table 1). The signal intensity of the covalent drug–DNA complex at 12 627 Da (Figure 4B) compared favourably to the peak intensity of the corresponding covalent pixantrone–dsBE12 complex (12 569 Da peak of Figure 4A), indicating that the binding of activated pixantrone to the methylated duplex dsBE67 was enhanced relative to the unmethylated duplex dsBE12.

A second cluster of peaks was also observed in the 12 940–70 Da mass range of the spectra presented

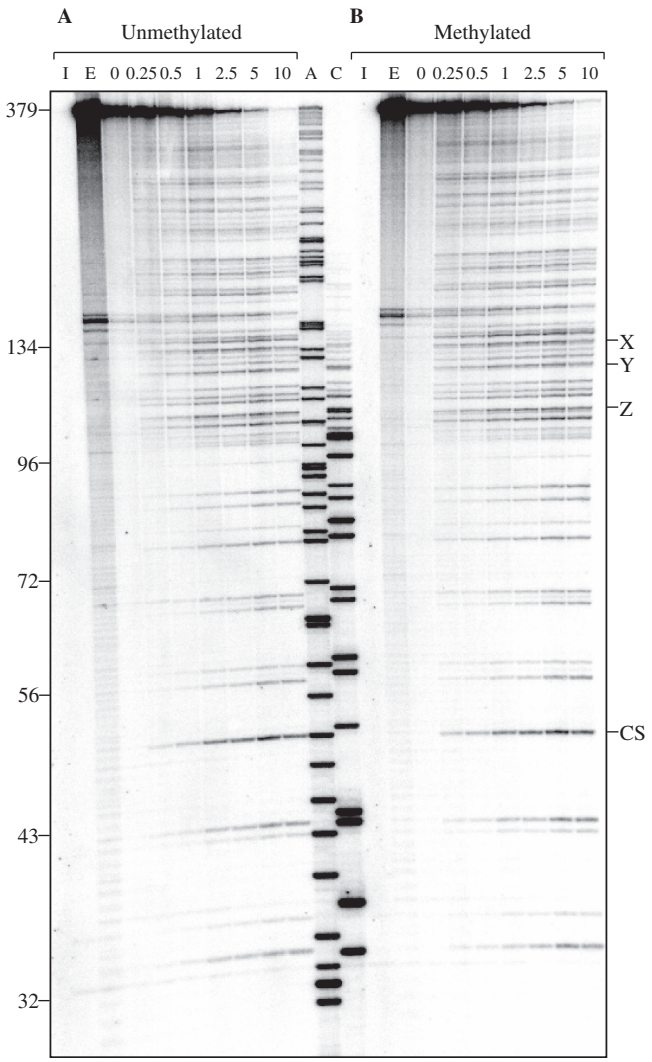

Figure 2. Drug-induced transcriptional blockages are *not* enhanced at discrete MspI-methylated sequences. (**A**) A native 512 bp DNA fragment (25 μM_{bp}) was treated with pixantrone (0–10 μM as indicated) and 2 mM formaldehyde for 4 h. Drug-treated templates were subsequently subjected to *in vitro* transcription, electrophoresis and finally phosphorimaging. Controls are as described in Figure 1. (**B**) The native 512 bp fragment in (A) was substituted for an identical fragment specifically methylated by MspI methylase at the external cytosine of each CCGG recognition sequence. The MspI-methylated fragment was then reacted with drug and subjected to transcription as described in (A). Three MspI-methylated sites are indicated by X, Y and Z at the right of the phosphorimage. CS denotes an unmethylated CpG control site. The mole fraction of blockages at MspI-methylated sites X, Y and Z and at an unmethylated control site (CS), were quantitated and are expressed as a function of pixantrone concentration in (**C**), (**D**), (**E**) and (**F**), respectively. Unmethylated and methylated 512 bp DNA substrates are denoted by solid and open squares, respectively.

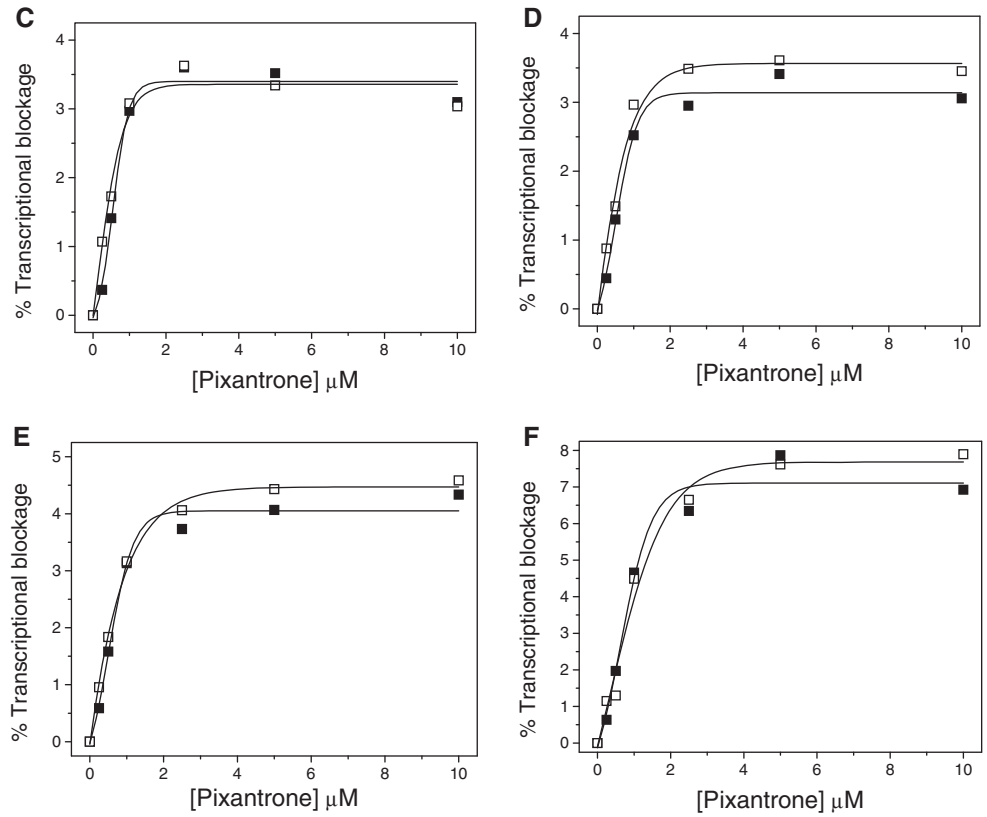

Figure 2. Continued.

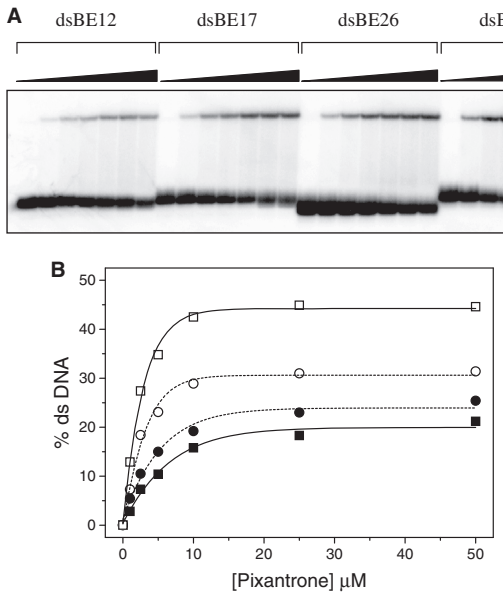

Figure 3. Pixantrone–DNA adduct induced stabilization of synthetic oligonucleotides containing 5-methyl-deoxycytosine as assessed by a gel shift assay. (**A**) Various oligonucleotides substrates ($25\,\mu M_{bp}$) including unmethylated dsBE12, hemi-methylated dsBE17 and dsBE26 and fully methylated dsBE67 were incubated with either 0, 1, 2.5, 5, 10, 25 or 50 μM pixantrone (denoted by a solid triangle) and 2 mM formaldehyde overnight at 37°C in PBS (pH 7.0). Drug-treated samples were then subjected to denaturing PAGE and phosphorimaging. (**B**) The relative amount of dsDNA represented in (A) was quantitated and is expressed as a function of pixantrone concentration (dsBE12, solid line, solid squares; dsBE67, solid line, open squares; dsBE26, dashed line, solid circles; dsBE17, dashed line, open circles).

in Figure 4B. The first and smallest of these signals at 12 939 Da (Figure 4B) is consistent with dsBE67 accommodating intercalation by two pixantrone molecules (Table 1). The second and third peaks of this cluster increased in multiples of 12–13 Da (Figure 4B) and are representative of the generation of one pixantrone–DNA adduct (and one intercalated pixantrone) or two pixantrone–DNA adducts (Table 1).

Pixantrone–DNA adduct stability is modestly influenced by localized CpG methylation and only at select sequences

A marked and consistent enhancement in the generation of covalent pixantrone–DNA adducts by CpG methylation prompted an investigation into the permanence of these lesions at discretely methylated sites. The transcription assay is ideal for the specific measurement of covalent pixantrone–DNA adducts without interference by non-covalent pixantrone–DNA interactions (7). Following reaction with formaldehyde and pixantrone, either native or methylated drug-reacted 512 bp DNA templates were subjected to transcriptional elongation for up to 4 h. The phosphorimage presented in Figure 5 shows the effect of HpaII methylation (CCm^5GG) on the decay of transcriptional blockages with increasing elongation times. The fraction of transcriptional blockages at individual sites X, Y and Z was quantitated for each entire lane of Figure 5 and the persistence of these adducts, expressed as a half-life at each site, is summarized in Table 2. An assessment of the data presented in Table 2 suggests that the stability of pixantrone–DNA adducts at CCGG sites is

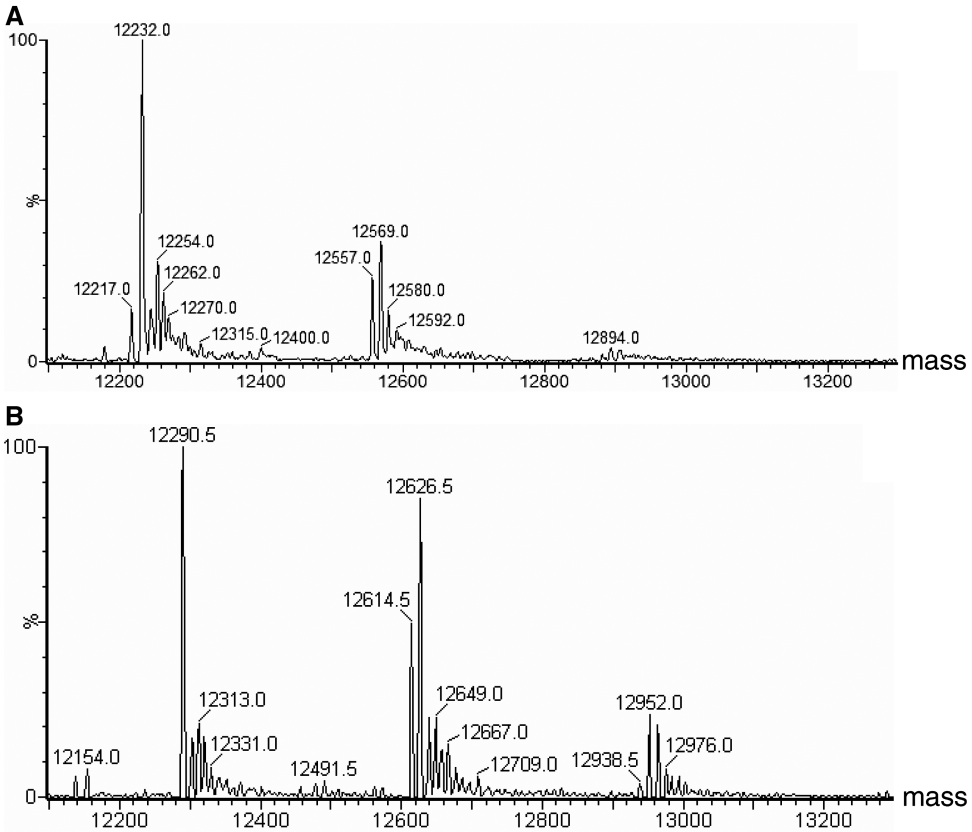

Figure 4. Mass spectrometric analysis of oligonucleotide duplexes dsBE12 and dsBE67. The oligonucleotide duplexes dsBE12 (**A**) and dsBE67 (**B**) were incubated with 10 mM formaldehyde and 100 μM pixantrone in PBS (pH 7.0) at 37°C overnight. Drug–oligonucleotide complexes were subsequently processed and subjected to mass spectrometry as described in the 'Materials and Methods' section. The spectra are expressed as a function of absolute molecular mass (Da).

Table 1. The expected and observed masses for each major peak depicted in Figure 4

Figure 4	Reaction conditions	Products	Expected mass (Da)	Observed mass (Da)
A	10 mM formaldehyde + 100 μM pixantrone	dsBE12	12 232	12 232
		+(1× Pix_{int})	12 557	12 557
		+(1× Pix_{add})	12 569	12 569
B	10 mM formaldehyde + 100 μM pixantrone	dsBE67	12 288	12 291
		+(1× Pix_{int})	12 613	12 615
		+(1× Pix_{add})	12 625	12 627
		+(2× Pix_{int})	12 938	12 939
		+(1× Pix_{int}) + (1× Pix_{add})	12 950	12 952
		+(2× Pix_{add})	12 962	12 964

The abbreviations Pix_{int} and Pix_{add} denote the intercalated species of pixantrone and the pixantrone–DNA adduct, respectively. The molecular mass of pixantrone is 325 Da.

only modestly enhanced by methylation at the internal cytosine residue of the sequence. Moreover, methylation of the external cytosine of the same recognition sequence (Cm^5CGG) by MspI methylase had no significant influence on the stability of pixantrone–DNA adducts (Table 2).

A gel shift assay was subsequently employed to independently assess the stability of pixantrone–DNA adducts at CpG methylated sites. Both unmethylated dsBE12 and fully methylated dsBE67 oligonucleotide complexes were initially reacted with pixantrone and formaldehyde, subsequently purified to remove unreacted drug and the drug-oligonucleotide complex incubated at 37°C for defined time periods up to 180 min. The loss of pixantrone adducts from the oligonucleotide duplexes with time was monitored using a gel shift assay (Figure 6A). The fraction of duplex DNA remaining as double-stranded in Figure 6A was quantitated and is expressed as a function of time in Figure 6B. The dissociation of adducts from either unmethylated dsBE12 or methylated dsBE67 was identical, with pixantrone–DNA adducts in each duplex displaying half-lives of ~150 min.

DNA modification by cisplatin is unaffected by CpG methylation at localized CCGG (CCm^5GG) sequences

In an effort to further investigate the role of CpG methylation in drug–DNA damage, the covalent binding of cisplatin at HpaII-methylated CCGG (CCm^5GG) sites was analysed by *in vitro* transcription. Cisplatin (0–1 μM) was incubated with either a native or HpaII-methylated

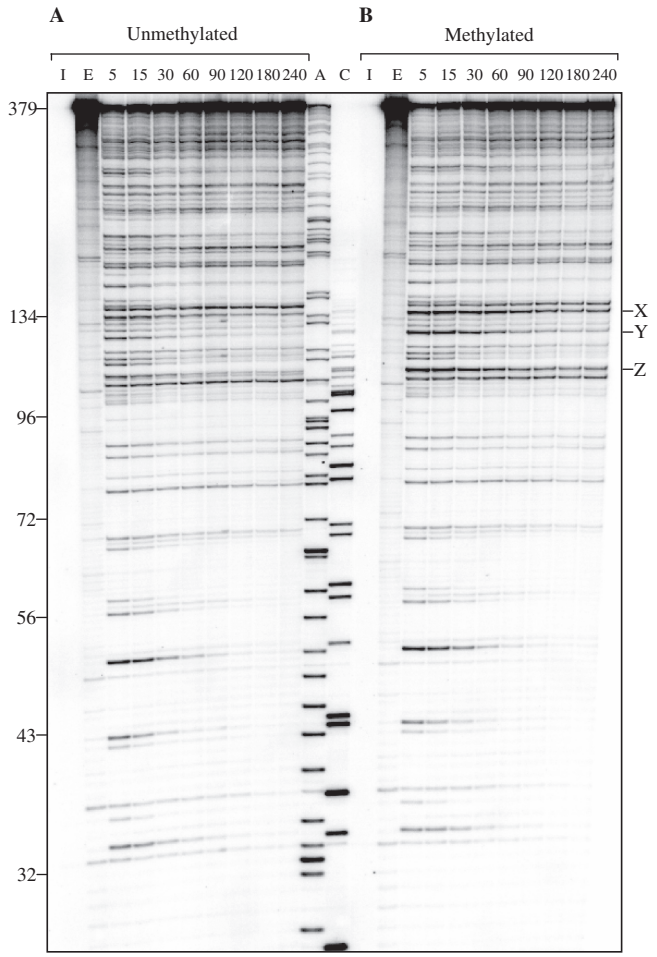

Figure 5. Elongation of the transcription complex past pixantrone-induced blockages at unmethylated CCGG and HpaII-methylated (CCm^5GG) sites. (**A**) The 512 bp fragment was initially reacted with 5 μM pixantrone and 2 mM formaldehyde for 4 h. Following ethanol precipitation, drug-reacted DNA was resuspended and transcription initiated from the *lac* UV5 promoter. Subsequent elongation of the initiated complex was allowed to proceed at 37°C for time periods ranging from 5 to 240 min. Controls are as stated in the legend of Figure 1. (**B**) The native 512 bp fragment in (A) was substituted for an identical fragment specifically methylated by HpaII methylase at the internal cytosine of each CCGG recognition sequence. The methylated fragment was subsequently reacted with drug and subjected to transcription as described in (A). CCGG recognition sites are indicated by X, Y and Z at the right of the phosphorimage.

Table 2. The stability of covalent pixantrone-DNA adducts at unmethylated CCGG sites versus HpaII-methylated (CCm^5GG) and MspI-methylated (Cm^5CGG) sequences

	HpaII methylation		MspI methylation	
Site	−Me	+Me	−Me	+Me
X	29 ± 4	53 ± 10	42 ± 9	34 ± 7
Y	18 ± 0.5	29 ± 0.5	22 ± 0.5	20 ± 2
Z	18 ± 1	22 ± 1	20 ± 1	21 ± 3

The stated values are the half-lives (in minutes) of adducts at each site and were determined by fitting the data to an exponential decay function (first order). The error associated with each value is the standard error of the fit. '−Me' and '+Me' represent unmethylated and methylated CCGG sites, respectively.

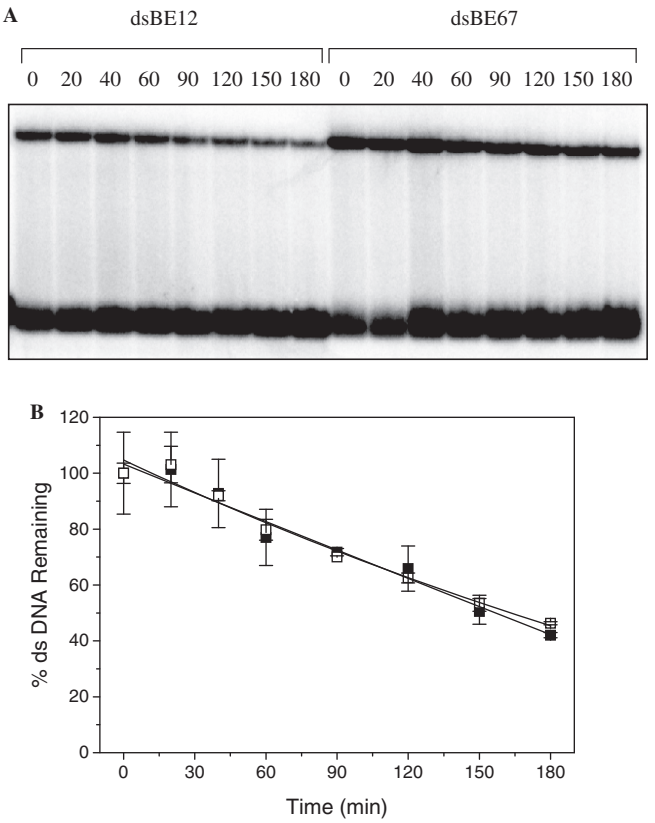

Figure 6. The stability of pixantrone–DNA adducts located within unmethylated and CpG methylated oligonucleotide duplexes. (**A**) [^{32}P]-End labelled duplexes (25 μM_{bp}) dsBE12 (unmethylated) and dsBE67 (methylated) were initially reacted with 50 μM pixantrone and 2 mM formaldehyde in PBS (pH 7.0) at 37°C overnight. Following the removal of unreacted drug, the covalent drug–DNA complex was incubated at 37°C for defined time periods up to 180 min (as indicated). Samples were then subjected to a gel shift assay as described in the 'Materials and Methods' section. (**B**) The fraction of DNA remaining as double stranded in (A) was quantitated and is expressed as a function of time (dsBE12, solid squares; dsBE67 open squares). Error bars represent the absolute maximum error of two independent experiments.

DNA fragment (25 μM_{bp}) in 0.5 × TE overnight at 37°C. Each drug-reacted template was subsequently subjected to *in vitro* transcription. The phosphorimage presented in Figure 7 indicates that cisplatin induced a clear dose-dependent decrease in full length transcript using both native and CCm^5GG-DNA templates. A concurrent increase in cisplatin-induced transcriptional blockages was also clearly evident (Figure 7A and B). Most importantly, a subset of these blockages occurred at CCGG sites within both DNA templates (indicated by X, Y and Z at the left of Figure 7A). Note that the blockages selectively occurred at the CpC of doublets of these sites (i.e. GpG dinucleotide sequence of the template strand). The relative occupancy of drug at sites X, Y and Z was quantitated as a fraction of each entire lane and is presented as a function of cisplatin concentration in Figure 7C–E. Clearly, the two curves of each graph represented in Figure 7 (unmethylated sites, solid squares; methylated DNA, open squares) closely coincide with each other, suggesting that the generation of cisplatin DNA adducts at each site was unaffected at localized

CCm^5GG sequences. The frequency of transcriptional blockages at a non-CCGG binding site (denoted CS at the left of Figure 7A) was also quantitated and is displayed as a function of cisplatin concentration in Figure 7F. This result suggests that there was no significant difference in the generation of cisplatin adducts using the two different DNA templates.

DNA alkylation by the formaldehyde-activated anthracyclines doxorubicin and epirubicin is selectively enhanced at HhaI-methylated (GCm^5GC) sites

The effect of CpG methylation on the alkylation of DNA by formaldehyde-activated doxorubicin was subsequently investigated within the 512 bp DNA fragment. Each GCGC site within the 512 bp fragment was specifically methylated at the internal cytosine residue by HhaI methylase (denoted GCm^5GC). Methylation at these sites incorporates *both* the natural substrate of DNA methylation in the CpG doublet *and* two contiguous GpC dinucleotides, the favoured binding site of formaldehyde-activated doxorubicin. Clearly, this unique permutation of nucleotides provides an ideal experimental opportunity to investigate the potential modulation of doxorubicin–DNA damage by CpG methylation.

Following reaction with formaldehyde (1 mM) and doxorubicin (0–250 nM), the native, unmethylated 512 bp DNA fragment was subjected to *in vitro* transcription from the *lac* UV5 promoter. Transcription of the template yields a pattern of blockages (Figure 8A) that are consistent with a typical footprint induced by formaldehyde-activated doxorubicin (7). Drug-reacted templates bearing methylated GCm^5GC sequences generated an identical profile of transcriptional blockages (Figure 8B), however the intensity of blockages at each GCm^5GC site (denoted by U, V and W at the right of Figure 8B) is greater relative to the equivalent sites in the native, unmethylated fragment (Figure 8A). The extent of drug-induced blockages at sites U, V and W were quantitated as a fraction of transcripts in each lane and are represented as a function of doxorubicin concentration (Figure 8C–E). A clear 2–3-fold increase in blockage intensity at each GCm^5GC site relative to the corresponding unmethylated sequence is evident (Figure 8C–E). An unmethylated GpC site alkylated by formaldehyde-activated doxorubicin (denoted CS at the right of Figure 8B) was quantitated as a control (Figure 8F) to demonstrate that there was no significant difference in doxorubicin–DNA adduct formation at unmethylated GpC doublets using the two different DNA templates.

A similar enhancement in DNA alkylation was also displayed by formaldehyde-activated epirubicin, another GpC-specific alkylator, at HhaI-methylated sites (Supplementary Figure S3). The CpG methylation-mediated enhancement of drug-induced blockages at site U was especially pronounced (by up to 9-fold), while the increase at sites V and W were more modest (by 2–3-fold), but still significant (Supplementary Figure S4). Again, an unmethylated GpC site was quantitated and showed no significant difference in its alkylation by activated epirubicin on the two independent templates (Supplementary Figure S4).

Pixantrone and doxorubicin-induced growth inhibition in wildtype versus HCT116DKO cells

The growth inhibitory effect of pixantrone on HCT116 wildtype and HCT116DKO cells is presented in

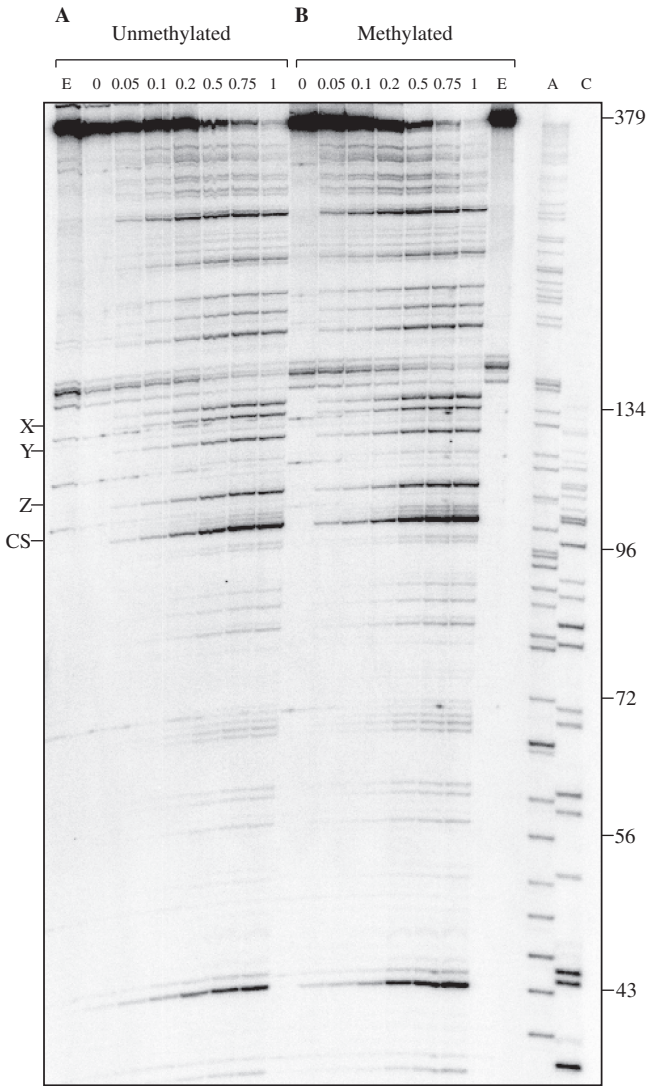

Figure 7. The effect of CpG methylation on cisplatin-induced transcriptional blockages at neighbouring CpC sequences. Cisplatin (0–1 μM as indicated) was initially reacted with either (**A**) an unmethylated or (**B**) a HpaII-methylated 512 bp DNA fragment (25 μM_{bp}) overnight at 37°C. Drug-reacted templates were directly subjected to transcription as described in the legend of Figure 1. Controls are also as described in Figure 1. Three CCGG sites targeted by HpaII methylase are indicated by X, Y and Z at the left of the phosphorimage. CS denotes a non-CCGG site modified by cisplatin, but not methylated by HpaII methylase. The mole fraction of drug-induced blockages at native (solid squares) and methylated (open squares) CCGG sites X, Y and Z were quantitated as a fraction of each entire lane and are represented as a function of cisplatin concentration in (**C**), (**D**) and (**E**), respectively. (**F**) The % transcriptional blockage of the control site CS, a non-CCGG site modified by cisplatin but not methylated by HpaII methylase, was quantitated and is expressed as a function of cisplatin concentration.

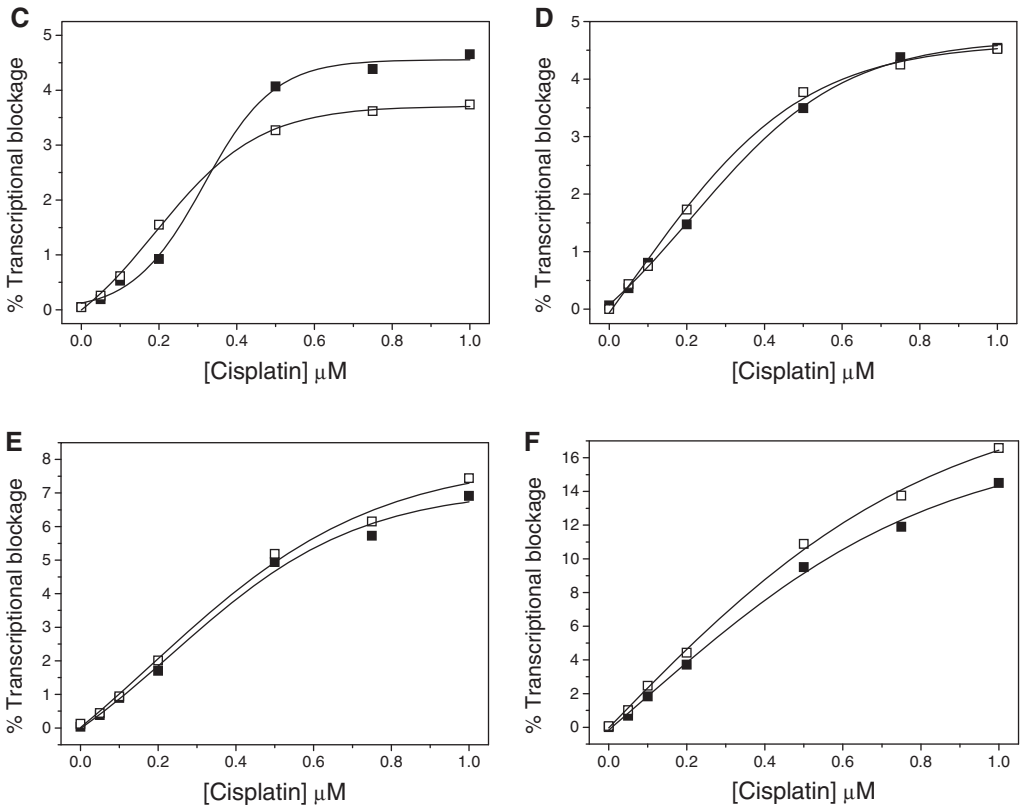

Figure 7. Continued.

Figure 9. The methylation depleted HCT116DKO cells displayed a 12-fold resistance to pixantrone, and a 10-fold resistance to doxorubicin. In contrast, this cell line was only ~2-fold resistant to cisplatin treatment compared to the wildtype HCT116 cells, and may be accounted at least in part by the comparatively slow growth rate of the HCT116DKO cells.

DISCUSSION

DNA methylation is a covalent epigenetic modification of the mammalian genome that can occur at each cytosine residue of the CpG motif. The modification assumes a critical role in both the regulation of gene expression and the development of cancer (8,12,23). In addition to being the predominant substrate of DNA methylation (8), the CpG doublet is also a target of numerous DNA damaging agents, including formaldehyde-activated pixantrone (7,9,24,25). Since the bulk of CpG dinucleotides are likely to be methylated *in vivo* (8,9,25–27), the present study initially examined the effect of localized CpG methylation on the alkylation of DNA by formaldehyde-activated pixantrone.

CpG methylation augments the generation of covalent pixantrone–DNA adducts

Three independent techniques, which included an *in vitro* transcription assay (Figure 1), an oligonucleotide band shift assay (Figure 3) and mass spectrometric analysis (Figure 4), all provided clear evidence that CpG methylation enhanced DNA alkylation by formaldehyde-activated pixantrone. Pixantrone joins an expanding catalogue of DNA-damaging agents that are susceptible to modulation by CpG methylation. Covalent modification of DNA by the chemical carcinogen *N*-methyl-*N*-nitrosourea (28) and UV-induced photoproducts (29,30) are both inhibited by proximal CpG methylation, yet other agents including the benzo[*a*]pyrene metabolite BPDE (24,31,32), aflatoxin B_1-8,9-epoxide (33) and the therapeutic agents mitomycin C (9,21,34), esperamicins A1 and C (25) and formaldehyde-activated mitoxantrone (35,36) are all enhanced at methylated CpG dinucleotides. Given that each of these latter DNA-interactive agents (excluding the esperamicins A1 and C) alkylate DNA via the guanine residue of CpG doublets and are enhanced by methylation at the 5′ neighbouring cytosine, it would be appealing to establish if these compounds and formaldehyde-activated pixantrone share a common reaction mechanism in their alkylation of the methylated CpG motif.

Modulation of DNA binding by CpG methylation is not a general feature of all alkylators

Activated doxorubicin strongly favours DNA alkylation at GpC steps (7,37–40), yet the intercalated species of the drug and other closely-related anthracyclines prefer

binding at the isomeric CpG doublet (41,42). Merging the two dinucleotide sequences together yields the triplet GCG, a sequence which is represented in the HhaI methylase recognition site GCGC. Strikingly, when the central CpG step of this specific site was methylated by HhaI methylase, DNA alkylation by formaldehyde-activated doxorubicin was enhanced by 2 to 3-fold at neighbouring GpC sites (Figure 8). In contrast, the covalent binding of cisplatin at localized CCGG sequences was unaffected by methylation at the neighbouring central CpG step (Figure 7), suggesting that modulation of DNA binding by methylation may not be a general feature of adduct-forming agents. Rather, the structural feature that seems to confer an enhancement by CpG methylation is a flat, polycyclic ring system which permits non-covalent interactions within DNA. Thus, intercalation at methylated CpG steps may be a prerequisite for enhancement of covalent drug–DNA adducts.

A molecular rationale for the augmentation of pixantrone and doxorubicin–DNA damage at methylated CpG sites

Two distinct chemical mechanisms are generally considered in an effort to account for the enhancement of drug-induced DNA alkylation by CpG methylation. First, it has been suggested that cytosine methylation may increase the *chemical reactivity* of the N2 exocyclic amino group of guanine, through which mitomycin C, formaldehyde-activated mitoxantrone, BPDE and formaldehyde-activated pixantrone covalently bind to DNA (7,31,34,36). The N2 amino function of guanine may be made more nucleophilic by the neighbouring methyl group of the 5-methylcytosine via an electron-donating effect (24,34,43). The credibility of this idea has been challenged since the methyl group of cytosine extends into the major groove of DNA, quite distal to the reactive N2 amino centre of guanine within the minor groove (31). Moreover, Chen *et al.* (33) established that CpG methylation augments DNA alkylation by a range of bulky carcinogens, which covalently bind through guanine at a variety of reactive centres including N7 and C8 positions of the base, not just the N2 centre. Such a result cannot be attributed to an increase in the nucleophilicity of a single reactive centre and suggests that a broader, less specific mechanism may be responsible for the enhancement of drug-induced DNA alkylation by CpG methylation.

An alternative mechanism involves a shift in the initial structural *accessibility* of the alkylator by CpG methylation to a more favourable position for the generation of a covalent bond with DNA. It is well established that CpG methylation induces numerous conformational alterations in the local structure of duplex DNA that include enhancing the transition of DNA from B to Z forms, increasing helical pitch and unwinding and influencing the formation of DNA cruciforms, a unique DNA secondary structure (21,44–48). By coincidence, Vargason *et al.* (49) characterized the effect of CpG methylation on the hexamer d(GGCGCC)$_2$, a sequence repeated twice within the 512 bp fragment used in the present study for *in vitro* transcription. Pixantrone–DNA alkylation was enhanced at both of these sequences in HhaI-methylated templates (Supplementary Figure S2). CpG methylation in the context of the hexamer d(GGC GCC)$_2$ induces a conformational change in the duplex that is representative of a transition state from B-DNA to A-DNA (49). Features specific to this unique duplex,

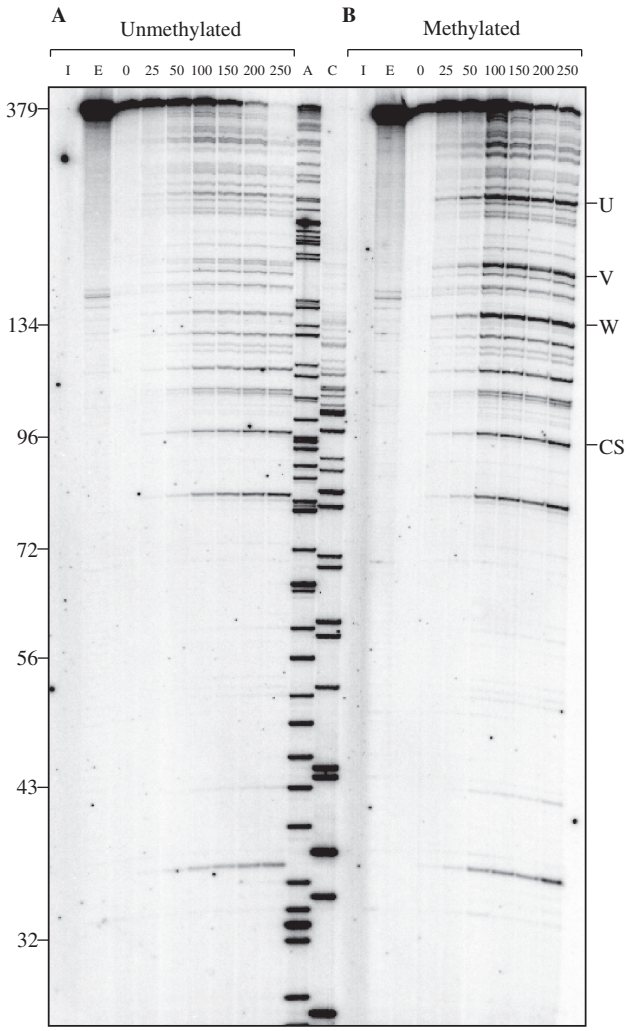

Figure 8. Multiple blocked transcripts induced by doxorubicin–DNA adducts at discrete HhaI-methylated sequences. (**A**) An unmethylated 512 bp DNA fragment (25 μM_{bp}) was initially incubated with 0–250 nM doxorubicin (as indicated) and 1 mM formaldehyde for 4 h at 37°C. Each reaction was terminated by ethanol precipitation and drug-reacted samples subsequently resuspended and subjected to transcription as described in the legend of Figure 1. Controls are as described in Figure 1. (**B**) The native 512 bp DNA fragment in (A) was substituted for an identical fragment specifically methylated by HhaI methylase at the internal cytosine of each GCGC recognition sequence. The HhaI-methylated fragment was subsequently reacted with drug and subjected to transcription as described in (A). Three GCGC sites, targeted by HhaI methylase, are indicated by U, V and W at the right of the phosphorimage. CS represents an unmethylated GpC site alkylated by formaldehyde-activated doxorubicin. The amount of RNA transcript at unmethylated (solid squares) and methylated (open squares) U, V and W sites was quantitated and is expressed as a function of doxorubicin concentration in (**C**), (**D**) and (**E**), respectively. (**F**) The mole fraction of RNA transcript at control site CS, a GpC site not methylated by HhaI methylase, was quantitated and is expressed as a function of doxorubicin concentration.

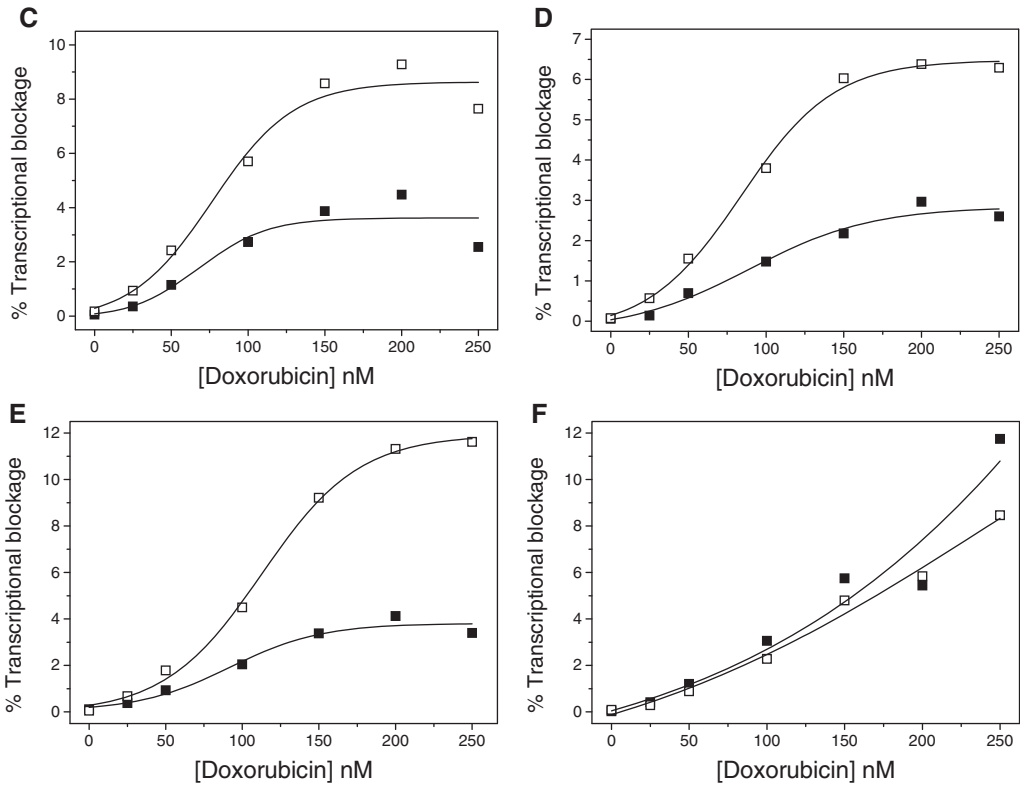

Figure 8. Continued.

such as an extended helical rise (49), may facilitate the enhancement of pixantrone–DNA adducts observed at these sequences.

The methyl moiety of 5-methylcytosine protrudes sterically out into the hydrophilic major groove of duplex DNA and imparts an element of hydrophobicity to its proximal region (47) and this may be pertinent to DNA alkylators that also interact with DNA via non-covalent intercalation, a mode of binding that is distinct from their capacity to covalently modify DNA. The benzo[*a*]pyrene metabolite BPDE, 2,7-diaminomitosene (a primary mitomycin C metabolite) and mitoxantrone are three examples of agents that display both modes of DNA binding in the appropriate environment. Interestingly, the non-covalent intercalative binding of all three are significantly enhanced by methylated CpG DNA (36,50,51), suggesting that methylation-enhanced drug–DNA intercalation may be a precursor to increased drug–DNA alkylation.

A further indication that localized CpG methylation may enhance initial drug intercalation is provided by *in vitro* transcription studies of the MspI-methylated template (Figure 2). MspI methylation at the external cytosine residues of CCGG sites failed to enhance formaldehyde-activated pixantrone DNA alkylation (Figure 2), indicating that the methyl substituents must be positioned at the internal cytosine residues of the recognition motif to augment DNA alkylation. Presumably, the internal CpG site of the recognition sequence CCGG is also the site of initial intercalation of pixantrone.

Molecular modelling analysis of the mitoxantrone–DNA intercalation complex has demonstrated that CpG methylation essentially shifts the distribution of intercalated drug from the major to the minor groove (36). The methyl moiety of 5-methylcytosine may achieve this shift in equilibrium by sterically protruding out into the major groove, thereby impairing drug entry. Once positioned within the minor groove of DNA, the drug is ideally situated for covalent reaction with the adjacent N2 amino group of guanine, the established site of DNA alkylation by formaldehyde-activated mitoxantrone (36). Given their strong structural similarity, formaldehyde-mediated mitoxantrone, doxorubicin and pixantrone–DNA alkylation are most likely to be enhanced by CpG methylation via highly analogous mechanisms.

The generation of CpG selective pixantrone–DNA adducts may impair the activity of DNMTs, which specifically target the doublet

A consistent feature of almost every tumour type is their tendency to accommodate a large range of tumour suppressor and cancer-related genes that are characteristically silenced by CpG methylation in their promoter regions (12,15). These cancer-specific methylation patterns must be actively maintained between cell generations by DNMTs for progenitor cells to retain their survival advantage (15,52). Therapeutically disrupting the transmission of cancer-associated methylation patterns enables the reactivation of once-dormant tumour suppressor

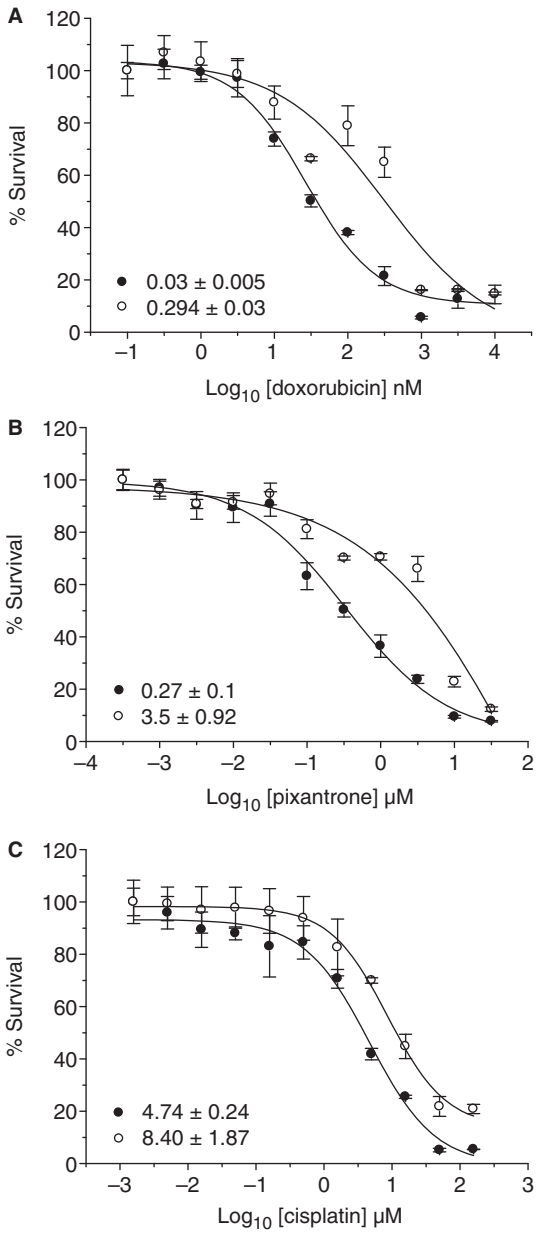

Figure 9. Representative growth inhibition curves of HCT116 (closed circles) and HCT116DKO (open circles) cells as determined by an MTT assay after 72 h treatment with doxorubicin (**A**), pixantrone (**B**) or cisplatin (**C**). Error bars represent the standard deviation of four replicates of a single typical experiment. The inset indicates the IC_{50} value (μM) of each drug and the error represents the standard deviation of at least three independent experiments.

genes (47). Moreover, the reversible nature of DNA methylation suggests that this can be achieved without altering the DNA sequence (53,54). A distinctive feature of the methylation-enhanced generation of pixantrone–DNA adducts is that hemi-methylation is sufficient to induce a significant 1.25–2.5-fold increase in DNA alkylation by these lesions (Figure 3). Pixantrone–DNA adduct formation at both unmethylated and hemi-methylated CpG doublets has potential biological implications, since these particular sequences are also receptors of cellular DNMTs.

Historically, the inhibition of DNA methylation and gene reactivation as therapeutic targets has been achieved using the nucleoside analogues 5-aza-2′-deoxycytidine and 5-aza-cytidine (12,52,55,56). Nucleosides such as these induce their cytotoxic properties by poisoning DNMTs following their incorporation into DNA (52,56). The development of nucleosides as therapeutic compounds has been impaired primarily by their inherent toxicity, a characteristic commonly attributed to their non-specific incorporation into DNA (52,55,56). The deleterious nature of these compounds has placed an emphasis on the development of non-nucleoside inhibitors of DNMTs. A handful of such molecules have recently been identified and described. Procainamide and procaine are two small molecule 4-aminobenzoic acid derivatives that inhibit DNMT activity, an outcome that may be attributed to their strong binding to DNA rich in the CpG motif (52,55,56). Both agents induce global and localized CpG island-demethylation and re-expression of the associated genes in a cellular environment (55,57) and these effects may contribute towards their growth inhibitory properties. Similarly, formaldehyde-activated mitoxantrone, a close structural analogue of pixantrone, can also mediate localized demethylation of CpG islands in several cancer-associated genes (58). A functional consequence of this demethylation was the reactivation of the associated gene.

The CpG specific alkylator BPDE provides a further interesting example. It is well established that BPDE-modified DNA is a poor substrate for methylation catalysed by highly purified maintenance and *de novo* DNA methylases and DNMTs *in vitro* (59–61), suggesting that BPDE inhibits the activity of these enzymes. Within a cellular environment, benzo[*a*]pyrene, the metabolic precursor of BPDE, has been reported to induce a significant decrease in global content of 5-methylcytosine (62,63). More specifically, the carcinogen can induce hypomethylation at localized genomic repeats (64) and elicit changes in cellular gene expression in a time and dose-dependent manner (65).

The CpG selective nature of formaldehyde-activated pixantrone may help confer the drug with the properties necessary for inhibiting DNMTs. Despite their obvious differences, the common DNA-damaging attributes shared by benzo[*a*]pyrene and formaldehyde-activated pixantrone suggests that pixantrone may generate similar cellular responses worthy of investigation. Clearly, they include the potential reactivation of silenced cancer-related genes by DNA demethylation and the inhibition of DNMTs *in vivo*.

The enhancement of pixantrone–DNA and doxorubicin–DNA lesions at methylated CpG doublets may confer a selective toxicity in certain cancers

Endogenous levels of formaldehyde have previously been shown to be sufficient for the formation of doxorubicin–DNA adducts in MCF-7 cells (66). Since many tumours have characteristically elevated formaldehyde levels (67,68) this provides an environment for the formation of doxorubicin and pixantrone–DNA adducts.

The biological significance of the methylation-mediated enhancement of pixantrone- and doxorubicin–DNA lesions was addressed through the use of HCT116DKO colon cancer cells vastly deficient in genomic DNA methylation (69). These cells, retaining just 5% of the genomic DNA methylation content of their parental line (69), were 12- and 10-fold more resistant to pixantrone- and doxorubicin-induced growth inhibition, respectively (Figure 9), suggesting higher levels of genomic CpG methylation may be a determinant in the cytotoxicity of these drugs. In contrast, cisplatin, a drug insensitive to CpG methylation *in vitro* (Figure 7), induced only a marginal 2-fold difference in growth inhibition (Figure 9). The minor cisplatin-induced differential in growth inhibition hints that the drug may not be sensitive to the DNA methylation profile of a given cell type, consistent with *in vitro* data (Figure 7).

The use of the methylation-deficient HCT116DKO cells highlights that differential genomic CpG methylation patterns may have significant implications for pixantrone- and doxorubicin-induced cell death. The challenge now is to refine this relationship and establish if a characteristic pattern of CpG methylation, or 'methylome', engenders a cancer with a particular susceptibility to these agents.

SUPPLEMENTARY DATA

Supplementary Data are available at NAR Online.

FUNDING

National Health and Medical Research Council, Australia [grant number 487333] [to S.M.C. and D.R.P.] and CASS foundation, Melbourne, Australia [grant number SM/08/1971] [to S.M.C.]. Funding for open access charge: University allowance.

Conflict of interest statement. None declared.

REFERENCES

1. Faulds,D., Balfour,J.A., Chrisp,P. and Langtry,H.D. (1991) Mitoxantrone. A review of its pharmacodynamic and pharmacokinetic properties, and therapeutic potential in the chemotherapy of cancer. *Drugs*, **41**, 400–449.
2. Hazlehurst,L.A., Krapcho,A.P. and Hacker,M.P. (1995) Correlation of DNA reactivity and cytotoxicity of a new class of anticancer agents: aza-anthracenediones. *Cancer Lett*., **91**, 115–124.
3. De Isabella,P., Palumbo,M., Sissi,C., Capranico,G., Carenini,N., Menta,E., Oliva,A., Spinelli,S., Krapcho,A.P., Giuliani,F.C. *et al*. (1995) Topoisomerase II DNA cleavage stimulation, DNA binding activity, cytotoxicity, and physico-chemical properties of 2-aza- and 2-aza-oxide-anthracenedione derivatives. *Mol. Pharmacol*., **48**, 30–38.
4. Hazlehurst,L.A., Krapcho,A.P. and Hacker,M.P. (1995) Comparison of aza-anthracenedione-induced DNA damage and cytotoxicity in experimental tumor cells. *Biochem. Pharmacol*., **50**, 1087–1094.
5. Zwelling,L.A., Mayes,J., Altschuler,E., Satitpunwaycha,P., Tritton,T.R. and Hacker,M.P. (1993) Activity of two novel anthracene-9,10-diones against human leukemia cells containing intercalator-sensitive or -resistant forms of topoisomerase II. *Biochem. Pharmacol*., **46**, 265–271.
6. Evison,B.J., Mansour,O.C., Menta,E., Phillips,D.R. and Cutts,S.M. (2007) Pixantrone can be activated by formaldehyde to generate a potent DNA adduct forming agent. *Nucleic Acids Res*., **35**, 3581–3589.
7. Evison,B.J., Chiu,F., Pezzoni,G., Phillips,D.R. and Cutts,S.M. (2008) Formaldehyde-activated Pixantrone is a monofunctional DNA alkylator that binds selectively to CpG and CpA doublets. *Mol. Pharmacol*., **74**, 184–194.
8. Laird,P.W. (2003) The power and the promise of DNA methylation markers. *Nat. Rev. Cancer*, **3**, 253–266.
9. Millard,J.T. and Beachy,T.M. (1993) Cytosine methylation enhances mitomycin C cross-linking. *Biochemistry*, **32**, 12850–12856.
10. Robertson,K.D. and Wolffe,A.P. (2000) DNA methylation in health and disease. *Nat. Rev. Genet*., **1**, 11–19.
11. Jones,P.A. and Baylin,S.B. (2002) The fundamental role of epigenetic events in cancer. *Nat. Rev. Genet*., **3**, 415–428.
12. Momparler,R.L. and Bovenzi,V. (2000) DNA methylation and cancer. *J. Cell Physiol*., **183**, 145–154.
13. Melki,J.R., Vincent,P.C. and Clark,S.J. (1999) Concurrent DNA hypermethylation of multiple genes in acute myeloid leukemia. *Cancer Res*., **59**, 3730–3740.
14. Santos,K.F., Mazzola,T.N. and Carvalho,H.F. (2005) The prima donna of epigenetics: the regulation of gene expression by DNA methylation. *Braz. J. Med. Biol. Res*., **38**, 1531–1541.
15. Esteller,M. (2002) CpG island hypermethylation and tumor suppressor genes: a booming present, a brighter future. *Oncogene*, **21**, 5427–5440.
16. Esteller,M., Corn,P.G., Baylin,S.B. and Herman,J.G. (2001) A gene hypermethylation profile of human cancer. *Cancer Res*., **61**, 3225–3229.
17. Esteller,M. (2007) Epigenetic gene silencing in cancer: the DNA hypermethylome. *Hum. Mol. Genet*., **16(Spec No 1)**, R50–R59.
18. Costello,J.F., Fruhwald,M.C., Smiraglia,D.J., Rush,L.J., Robertson,G.P., Gao,X., Wright,F.A., Feramisco,J.D., Peltomaki,P., Lang,J.C. *et al*. (2000) Aberrant CpG-island methylation has non-random and tumour-type-specific patterns. *Nat. Genet*., **24**, 132–138.
19. Paz,M.F., Fraga,M.F., Avila,S., Guo,M., Pollan,M., Herman,J.G. and Esteller,M. (2003) A systematic profile of DNA methylation in human cancer cell lines. *Cancer Res*., **63**, 1114–1121.
20. Shen,L., Kondo,Y., Ahmed,S., Boumber,Y., Konishi,K., Guo,Y., Chen,X., Vilaythong,J.N. and Issa,J.P. (2007) Drug sensitivity prediction by CpG island methylation profile in the NCI-60 cancer cell line panel. *Cancer Res*., **67**, 11335–11343.
21. Li,V.S., Reed,M., Zheng,Y., Kohn,H. and Tang,M. (2000) C5 cytosine methylation at CpG sites enhances sequence selectivity of mitomycin C-DNA bonding. *Biochemistry*, **39**, 2612–2618.
22. Wallace,R.B. and Miyada,C.G. (1987) Oligonucleotide probes for the screening of recombinant DNA libraries. *Methods Enzymol*., **152**, 432–442.
23. Herman,J.G. (1999) Hypermethylation of tumor suppressor genes in cancer. *Semin. Cancer Biol*., **9**, 359–367.
24. Yoon,J.H., Smith,L.E., Feng,Z., Tang,M., Lee,C.S. and Pfeifer,G.P. (2001) Methylated CpG dinucleotides are the preferential targets for G-to-T transversion mutations induced by benzo[a]pyrene diol epoxide in mammalian cells: similarities with the p53 mutation spectrum in smoking-associated lung cancers. *Cancer Res*., **61**, 7110–7117.
25. Mathur,P., Xu,J. and Dedon,P.C. (1997) Cytosine methylation enhances DNA damage produced by groove binding and intercalating enediynes: studies with esperamicins A1 and C. *Biochemistry*, **36**, 14868–14873.
26. Baylin,S.B., Herman,J.G., Graff,J.R., Vertino,P.M. and Issa,J.P. (1998) Alterations in DNA methylation: a fundamental aspect of neoplasia. *Adv. Cancer Res*., **72**, 141–196.
27. Bird,A.P. (1986) CpG-rich islands and the function of DNA methylation. *Nature*, **321**, 209–213.
28. Mathison,B.H., Said,B. and Shank,R.C. (1993) Effect of 5-methylcytosine as a neighboring base on methylation of DNA guanine by N-methyl-N-nitrosourea. *Carcinogenesis*, **14**, 323–327.
29. Pfeifer,G.P., Drouin,R., Riggs,A.D. and Holmquist,G.P. (1991) In vivo mapping of a DNA adduct at nucleotide resolution: detection of pyrimidine (6-4) pyrimidone photoproducts by

ligation-mediated polymerase chain reaction. *Proc. Natl Acad. Sci. USA*, **88**, 1374–1378.
30. Glickman,B.W., Schaaper,R.M., Haseltine,W.A., Dunn,R.L. and Brash,D.E. (1986) The C-C (6-4) UV photoproduct is mutagenic in Escherichia coli. *Proc. Natl Acad. Sci. USA*, **83**, 6945–6949.
31. Denissenko,M.F., Chen,J.X., Tang,M.S. and Pfeifer,G.P. (1997) Cytosine methylation determines hot spots of DNA damage in the human P53 gene. *Proc. Natl Acad. Sci. USA*, **94**, 3893–3898.
32. Tang,M.S., Zheng,J.B., Denissenko,M.F., Pfeifer,G.P. and Zheng,Y. (1999) Use of UvrABC nuclease to quantify benzo[a]pyrene diol epoxide-DNA adduct formation at methylated versus unmethylated CpG sites in the p53 gene. *Carcinogenesis*, **20**, 1085–1089.
33. Chen,J.X., Zheng,Y., West,M. and Tang,M.S. (1998) Carcinogens preferentially bind at methylated CpG in the p53 mutational hot spots. *Cancer Res.*, **58**, 2070–2075.
34. Johnson,W.S., He,Q.Y. and Tomasz,M. (1995) Selective recognition of the m5CpG dinucleotide sequence in DNA by mitomycin C for alkylation and cross-linking. *Bioorg. Med. Chem.*, **3**, 851–860.
35. Parker,B.S., Cutts,S.M. and Phillips,D.R. (2001) Cytosine methylation enhances mitoxantrone-DNA adduct formation at CpG dinucleotides. *J. Biol. Chem.*, **276**, 15953–15960.
36. Parker,B.S., Buley,T., Evison,B.J., Cutts,S.M., Neumann,G.M., Iskander,M.N. and Phillips,D.R. (2004) A molecular understanding of mitoxantrone-DNA adduct formation: effect of cytosine methylation and flanking sequences. *J. Biol. Chem.*, **279**, 18814–18823.
37. Cullinane,C., van Rosmalen,A. and Phillips,D.R. (1994) Does adriamycin induce interstrand cross-links in DNA? *Biochemistry*, **33**, 4632–4638.
38. Cullinane,C. and Phillips,D.R. (1990) Induction of stable transcriptional blockage sites by adriamycin: GpC specificity of apparent adriamycin-DNA adducts and dependence on iron(III) ions. *Biochemistry*, **29**, 5638–5646.
39. Luce,R.A., Sigurdsson,S.T. and Hopkins,P.B. (1999) Quantification of formaldehyde-mediated covalent adducts of adriamycin with DNA. *Biochemistry*, **38**, 8682–8690.
40. Taatjes,D.J., Gaudiano,G., Resing,K. and Koch,T.H. (1996) Alkylation of DNA by the anthracycline, antitumor drugs adriamycin and daunomycin. *J. Med. Chem.*, **39**, 4135–4138.
41. Wang,A.H., Ughetto,G., Quigley,G.J. and Rich,A. (1987) Interactions between an anthracycline antibiotic and DNA: molecular structure of daunomycin complexed to d(CpGpTpApCpG) at 1.2-A resolution. *Biochemistry*, **26**, 1152–1163.
42. Chen,K.S., Gresh,N. and Pullman,B. (1986) A theoretical investigation on the sequence selective binding of adriamycin to double-stranded polynucleotides. *Nucleic Acids Res.*, **14**, 2251–2267.
43. Das,A., Tang,K.S., Gopalakrishnan,S., Waring,M.J. and Tomasz,M. (1999) Reactivity of guanine at m5CpG steps in DNA: evidence for electronic effects transmitted through the base pairs. *Chem. Biol.*, **6**, 461–471.
44. Hodges-Garcia,Y. and Hagerman,P.J. (1992) Cytosine methylation can induce local distortions in the structure of duplex DNA. *Biochemistry*, **31**, 7595–7599.
45. Zacharias,W., Jaworski,A. and Wells,R.D. (1990) Cytosine methylation enhances Z-DNA formation in vivo. *J. Bacteriol.*, **172**, 3278–3283.
46. Klysik,J., Stirdivant,S.M., Singleton,C.K., Zacharias,W. and Wells,R.D. (1983) Effects of 5 cytosine methylation on the B-Z transition in DNA restriction fragments and recombinant plasmids. *J. Mol. Biol.*, **168**, 51–71.
47. Zingg,J.M. and Jones,P.A. (1997) Genetic and epigenetic aspects of DNA methylation on genome expression, evolution, mutation and carcinogenesis. *Carcinogenesis*, **18**, 869–882.
48. Hodges-Garcia,Y. and Hagerman,P.J. (1995) Investigation of the influence of cytosine methylation on DNA flexibility. *J. Biol. Chem.*, **270**, 197–201.
49. Vargason,J.M., Eichman,B.F. and Ho,P.S. (2000) The extended and eccentric E-DNA structure induced by cytosine methylation or bromination. *Nat. Struct. Biol.*, **7**, 758–761.
50. Kumar,G.S., He,Q.Y., Behr-Ventura,D. and Tomasz,M. (1995) Binding of 2,7-diaminomitosene to DNA: model for the precovalent recognition of DNA by activated mitomycin C. *Biochemistry*, **34**, 2662–2671.
51. Geacintov,N.E., Shahbaz,M., Ibanez,V., Moussaoui,K. and Harvey,R.G. (1988) Base-sequence dependence of noncovalent complex formation and reactivity of benzo[a]pyrene diol epoxide with polynucleotides. *Biochemistry*, **27**, 8380–8387.
52. Stresemann,C., Brueckner,B., Musch,T., Stopper,H. and Lyko,F. (2006) Functional diversity of DNA methyltransferase inhibitors in human cancer cell lines. *Cancer Res.*, **66**, 2794–2800.
53. Brueckner,B., Boy,R.G., Siedlecki,P., Musch,T., Kliem,H.C., Zielenkiewicz,P., Suhai,S., Wiessler,M. and Lyko,F. (2005) Epigenetic reactivation of tumor suppressor genes by a novel small-molecule inhibitor of human DNA methyltransferases. *Cancer Res.*, **65**, 6305–6311.
54. Brueckner,B. and Lyko,F. (2004) DNA methyltransferase inhibitors: old and new drugs for an epigenetic cancer therapy. *Trends Pharmacol. Sci.*, **25**, 551–554.
55. Villar-Garea,A., Fraga,M.F., Espada,J. and Esteller,M. (2003) Procaine is a DNA-demethylating agent with growth-inhibitory effects in human cancer cells. *Cancer Res.*, **63**, 4984–4989.
56. Lee,B.H., Yegnasubramanian,S., Lin,X. and Nelson,W.G. (2005) Procainamide is a specific inhibitor of DNA methyltransferase 1. *J. Biol. Chem.*, **280**, 40749–40756.
57. Lin,X., Asgari,K., Putzi,M.J., Gage,W.R., Yu,X., Cornblatt,B.S., Kumar,A., Piantadosi,S., DeWeese,T.L., De Marzo,A.M. *et al.* (2001) Reversal of GSTP1 CpG island hypermethylation and reactivation of pi-class glutathione S-transferase (GSTP1) expression in human prostate cancer cells by treatment with procainamide. *Cancer Res.*, **61**, 8611–8616.
58. Parker,B.S., Cutts,S.M., Nudelman,A., Rephaeli,A., Phillips,D.R. and Sukumar,S. (2003) Mitoxantrone mediates demethylation and reexpression of cyclin d2, estrogen receptor and 14.3.3sigma in breast cancer cells. *Cancer Biol. Ther.*, **2**, 259–263.
59. Pfeifer,G.P., Grunberger,D. and Drahovsky,D. (1984) Impaired enzymatic methylation of BPDE-modified DNA. *Carcinogenesis*, **5**, 931–935.
60. Wojciechowski,M.F. and Meehan,T. (1984) Inhibition of DNA methyltransferases in vitro by benzo[a]pyrene diol epoxide-modified substrates. *J. Biol. Chem.*, **259**, 9711–9716.
61. Subach,O.M., Baskunov,V.B., Darii,M.V., Maltseva,D.V., Alexandrov,D.A., Kirsanova,O.V., Kolbanovskiy,A., Kolbanovskiy,M., Johnson,F., Bonala,R. *et al.* (2006) Impact of benzo[a]pyrene-2′-deoxyguanosine lesions on methylation of DNA by SssI and HhaI DNA methyltransferases. *Biochemistry*, **45**, 6142–6159.
62. Wilson,V.L. and Jones,P.A. (1983) Inhibition of DNA methylation by chemical carcinogens in vitro. *Cell*, **32**, 239–246.
63. Wilson,V.L. and Jones,P.A. (1984) Chemical carcinogen-mediated decreases in DNA 5-methylcytosine content of BALB/3T3 cells. *Carcinogenesis*, **5**, 1027–1031.
64. Sadikovic,B. and Rodenhiser,D.I. (2006) Benzopyrene exposure disrupts DNA methylation and growth dynamics in breast cancer cells. *Toxicol. Appl. Pharmacol.*, **216**, 458–468.
65. Hockley,S.L., Arlt,V.M., Brewer,D., Giddings,I. and Phillips,D.H. (2006) Time- and concentration-dependent changes in gene expression induced by benzo(a)pyrene in two human cell lines, MCF-7 and HepG2. *BMC Genomics*, **7**, 260.
66. Coldwell,K.E., Cutts,S.M., Ognibene,T.J., Henderson,P.T. and Phillips,D.R. (2008) Detection of Adriamycin-DNA adducts by accelerator mass spectrometry at clinically relevant Adriamycin concentrations. *Nucleic Acids Res.*, **36**, e100.
67. Spanel,P., Smith,D., Holland,T.A., Al Singary,W. and Elder,J.B. (1999) Analysis of formaldehyde in the headspace of urine from bladder and prostate cancer patients using selected ion flow tube mass spectrometry. *Rapid Commun. Mass Spectrom.*, **13**, 1354–1359.
68. Kato,S., Burke,P.J., Koch,T.H. and Bierbaum,V.M. (2001) Formaldehyde in human cancer cells: detection by preconcentration-chemical ionization mass spectrometry. *Anal. Chem.*, **73**, 2992–2997.
69. Rhee,I., Bachman,K.E., Park,B.H., Jair,K.W., Yen,R.W., Schuebel,K.E., Cui,H., Feinberg,A.P., Lengauer,C., Kinzler,K.W. *et al.* (2002) DNMT1 and DNMT3b cooperate to silence genes in human cancer cells. *Nature*, **416**, 552–556.